STEM CELLS®

DNA Methylation Profiles Define Stem Cell Identity and Reveal a Tight Embryonic–Extraembryonic Lineage Boundary

CLAIRE E. SENNER,[a,b] FELIX KRUEGER,[c] DAVID OXLEY,[d] SIMON ANDREWS,[c] MYRIAM HEMBERGER[a,b]

[a]Epigenetics Programme, [c]Bioinformatics Group, and [d]Mass Spectrometry Facility, The Babraham Institute, Cambridge, U.K.; [b]Centre for Trophoblast Research, University of Cambridge, Cambridge, U.K.

Key Words. Stem cells of the early embryo • Methylation profiles • Early cell lineages • Stem cell plasticity

ABSTRACT

Embryonic (ES) and epiblast (EpiSC) stem cells are pluripotent but committed to an embryonic lineage fate. Conversely, trophoblast (TS) and extraembryonic endoderm (XEN) stem cells contribute predominantly to tissues of the placenta and yolk sac, respectively. Here we show that each of these four stem cell types is defined by a unique DNA methylation profile. Despite their distinct developmental origin, TS and XEN cells share key epigenomic hallmarks, chiefly characterized by robust DNA methylation of embryo-specific developmental regulators, as well as a subordinate role of 5-hydroxymethylation. We also observe a substantial methylation reinforcement of pre-existing epigenetic repressive marks that specifically occurs in extraembryonic stem cells compared to in vivo tissue, presumably due to continued high *Dnmt3b* expression levels. These differences establish a major epigenetic barrier between the embryonic and extraembryonic stem cell types. In addition, epigenetic lineage boundaries also separate the two extraembryonic stem cell types by mutual repression of key lineage-specific transcription factors. Thus, global DNA methylation patterns are a defining feature of each stem cell type that underpin lineage commitment and differentiative potency of early embryo-derived stem cells. Our detailed methylation profiles identify a cohort of developmentally regulated sequence elements, such as orphan CpG islands, that will be most valuable to uncover novel transcriptional regulators and pivotal "gatekeeper" genes in pluripotency and lineage differentiation. STEM CELLS 2012;30:2732–2745

Disclosure of potential conflicts of interest is found at the end of this article.

INTRODUCTION

Stem cells are defined by their self-renewing capacity combined with the potential to differentiate into various cell types when exposed to the appropriate signals. However, the level of plasticity depends on the developmental stage of the progenitor population from which the stem cell is derived. During early development, the first definitive differentiation event after fertilization sets the trophectoderm (TE) layer of the blastocyst apart from cells of the inner cell mass (ICM). Subsequently, a layer of primitive endoderm (PE) cells delaminates from the ICM, while the remaining ICM cells form the epiblast [1]. These three cell populations constitute the first cell lineages of the early mouse embryo. Thus, the TE establishes the placental trophoblast cell lineage, the epiblast gives rise to the embryo proper, and PE cells form the extraembryonic endoderm (ExEnd) cell lineage that predominantly contributes to the visceral and parietal yolk sac layers [1, 2]. These developmental processes are driven by key transcription factors with lineage-determining capacity. Prime examples are CDX2 and EOMES that are confined to the TE layer of the blastocyst, NANOG,

OCT4 (encoded by the *Pou5f1* gene) and other pluripotency-associated genes in the ICM and epiblast, and GATA6, SOX17, GATA4, and SOX7 in the PE [3–6].

Each of the three cell lineages of the blastocyst and early postimplantation mouse embryo give rise to distinct stem cell lines: these are embryonic (ES) and epiblast (EpiSC) stem cells originating from cells of the epiblast, trophoblast stem (TS) cells from the TE, and extraembryonic endoderm stem (XEN) cells from the PE [7–11]. Each of these distinct stem cell types recapitulates the lineage-specific differentiation capacity of their precursors. Thus, in vitro and when reintroduced into chimeras, TS cells differentiate into the various trophoblast cell types of the placenta, XEN cells contribute predominantly to yolk sac tissues, and ES cells give rise to the embryo proper [8, 9, 12–14]. Like ES cells, EpiSCs are equally committed to an embryonic lineage fate and can differentiate into derivatives of all three germ layers in vitro and in teratomas, but they do not contribute to chimeras any longer [10, 11]. This loss of ground state (naïve) pluripotency is thought to correspond to their origin from a slightly later developmental stage of the postimplantation epiblast. Taken together, all four stem cell types of the early mouse embryo reflect the differentiation capacity of their progenitor cell

populations within the established lineage boundaries and are therefore regarded representative of the early cell lineages [2].

Cell lineage commitment at the late blastocyst stage depends on the establishment of an epigenetic cellular memory that puts stable lineage barriers in place. Lineage restriction coincides temporally with the acquisition of an asymmetric distribution of DNA methylation, in that the ICM is globally hypermethylated compared to the TE [15]. DNA methylation is generally considered a stable epigenetic modification that confers chromatin condensation and gene repression [16]. Lack of methylation due to genetic deficiency, for example, of the DNA methyltransferase *Dnmt1* leads to a loss of strict lineage commitment, enabling the ectopic differentiation of trophoblast derivatives from cells of the embryo proper and of ES cells [17]. We have previously identified the transcription factor *Elf5* as one key locus that confers this epigenetic control of cell fate restriction between the embryonic and trophoblast lineage. *Elf5* is hypomethylated and expressed in trophoblast cells where it reinforces commitment to the trophoblast lineage but it is methylated and stably repressed in ES and epiblast cells, thereby abrogating this pathway in cells of the embryonic lineage. Similarly, DNA methylation also controls the transition from a naïve to a primed state of pluripotency within the embryonic lineage by repressing *Dppa3* (also known as *Stella*) in EpiSCs, which normally prevents developmental reversal to an ES-like state [18].

Epigenetic regulation of "gatekeeper" genes like *Elf5* and *Dppa3* forms the basis for the canalization of developmental pathways, a concept famously suggested by Waddington [19]. Identification of such pivotal loci, as well as the relevance of prominent intragenic and intergenic methylation marks, is key to our understanding of how the differentiative plasticity of stem cells is controlled and how stable differentiation is progressively achieved. In this study, we set out to define the DNA methylation profiles of all four stem cell types of the early mouse embryo, that is, ES, EpiSC, TS, and XEN cells, with the aim to identify characteristic patterns and key target loci reflecting their lineage allocation and developmental potency. We find that despite their distinct origin, TS and XEN cells share an extraembryonic lineage signature that is markedly different from that of ES cells and EpiSCs. Our data also reveal a tight epigenetic regulation of lineage-specifying transcription factors defining each stem cell type, and provide important insights into gatekeeper genes that determine stem cell plasticity.

MATERIALS AND METHODS

Cell Culture

ES, TS, XEN, and EpiSC stem cell lines were cultured under standard conditions (see Supporting Information). Cell lines used were: ES, lines J1, E14, KH2, and PGK12.1 (a kind gift of Prof. N. Brockdorff, University of Oxford, U.K.); EpiSC, lines #5 and #9 (both a kind gift of Dr. P. Tesar, Case Western Reserve University, OH) and line PRG (a kind gift of Dr. P. Rugg-Gunn, The Babraham Institute, Cambridge, U.K.); TS, lines Rs26, GFP, and B6 (kind gifts of Dr. J. Rossant, Hospital for Sick Children, Toronto, Canada and Dr. A. Erlebacher, NY University School of Medicine, New York, USA); and XEN, lines IM8A1 (Dr. J. Rossant), #16, and E4 (Dr. P. Rugg-Gunn).

Embryos

All mice were maintained and treated under the Home Office's animals (scientific procedures) Act 1986. Pregnant females from natural matings of (C57BL/6 × CBA)F1 intercrosses were dissected at the gestational age indicated, counting the morning of

the vaginal plug as E0.5. Sexing embryos was carried out as described previously [20].

MeDIP-Seq

MeDIP-Seq was carried out as described previously [21]. Briefly, purified genomic DNA was sonicated to yield 150–600 bp fragments, and adaptors for paired-end sequencing (Illumina, San Diego, CA, USA, http://www.illumina.com) were ligated using NEB Next DNA Sample Prep Reagent Set 1 (New England Biolabs Hitchin, UK, http://www.neb.com). Immunoprecipitations (IPs) were carried out in triplicate using 500 ng DNA per sample, 1.25 μg anti-5-methylcytosine (anti-5mC) antibody (Eurogentec, Southhampton, UK, http://www.eurogentec.com), and 10 μl Dynabeads coupled with M-280 sheep anti-mouse IgG (Invitrogen, Carlsbad, CA, http://www.invitrogen.com). The three IPs were pooled and amplified for 12 cycles with adapter specific primers, run on a 1% agarose gel, and fragments ranging between 300 and 500 bp in size were cut out and purified using the Gel Elution Kit (Qiagen, Crawley, UK, http://www.qiagen.com) before cluster generation and sequencing. Sequencing was carried out on an Illumina Genome Analyzer GAIIX using Cluster Generation v2 and 4 chemistries as well as Sequencing by Synthesis Kits v3 and v4. Data collection was performed using Sequencing Control Software v2.5 and 2.6. Real-time Analysis 1.5-1.8 was used for base calling. Genomic mapping was performed using ungapped sequence_pair mode of ELAND in the Illumina CASAVA pipeline v1.5-1.8. Reads were mapped to the mouse genome build NCBIM37. Final data analysis was performed using SeqMonk software (www.bioinformatics.ac.uk/projects/) and DAVID [22, 23].

Mass Spectrometric Analysis

Genomic DNA was digested to individual nucleosides using DNA degradase Plus (Zymo Research, Irvine, CA, USA, http://www.zymoresearch.com). The nucleosides were analyzed by Liquid Chromatography - Mass Spectrometry/Mass Spectrometry (LC-MS/MS) on a Thermo LTQ Orbitrap mass spectrometer operated in selected reaction monitoring mode using higher energy c-trap dissociation (HCD) fragmentation, monitoring the transitions 228 > 112 (C), 242 > 126 (5mC), and 258 > 142 (5hmC). Absolute 5mC and 5hmC amounts were carefully calibrated against standards; all samples were analyzed in triplicate to sextuplicate.

Reverse Transcription and Quantitative Polymerase Chain Reaction (RT-qPCR)

Total RNA was extracted using Trizol reagent (Invitrogen). cDNA synthesis was typically performed on 2 μg RNA with H M-MuLV Reverse Transcriptase (Fermentas, Leon-Rot, Germany, http://www.fermentas.com) according to the manufacturer's instructions. Quantitative real time polymerase chain reaction (qPCR) was carried out using using SYBR Green Jump Start Ready Mix (Sigma Gillingham, UK, http://www.sigmaaldrich.com) on a Bio-Rad CFX-96 Real-Time PCR Detection System (Bio-Rad, Hemel Hempstead, UK, http://www.bio-rad.com). All primers are listed in the Supporting Information. Data were normalized against housekeeping reference genes *Sdha, Dynein*, *b-actin*, and *Idh2*.

Sequenom MassARRAY and Bisulphite Sequencing

DNA was bisulphite-treated using the Qiagen Epitect Kit following manufacturer's instructions. PCR products were cloned into the pGEM-T Easy vector (Promega, Madison, WI, http://www.promega.com) for sequencing or processed using the MassCLEAVE Kit (Sequenom, Hamburg, Germany, http://www.sequenom.com) for Sequenom MassARRAY analysis.

Flourescence in Situ Hybridisation (FISH)

Digoxygenin-11-dUTP (DIG)-labeled DNA *Xist* probes were generated by nick-translation from a plasmid containing the entire *Xist* cDNA sequence, using a DIG nick-translation mix (Roche

Diagnostics, Basel, Switzerland, http://www.roche-applied-science.com) according to the manufacturer's instructions. RNA-FISH was then carried out as described previously [24].

Immunostaining

Anti-5mC immunostaining was performed on 7 μm paraffin sections after pretreatment with 3N HCl, 0.1% Triton for 20–35 minutes. Detection was with anti-mouse AlexaFluor488 (Invitrogen) and nuclear counterstaining with bis-benzimide (Sigma). Images were taken on a Zeiss Meta confocal microscope.

RESULTS

Global DNA Methylation Levels in the Early Embryo and Its Distinct Stem Cell Types

To analyze how global DNA methylation levels in the four distinct stem cell types of the early embryo compare to each other, and to their in vivo tissue counterparts, we first performed immunostaining and mass spectrometric quantification of 5mC. The prominent lineage-specific methylation difference observed at the blastocyst stage between TE and ICM [15] was still evident several days postimplantation as we found less intense 5mC staining in the trophoblast compartment (composed of extraembryonic/chorionic ectoderm and ectoplacental cone) than in epiblast tissue at E7.5 (Fig. 1A). To accurately quantify 5mC levels in tissues and stem cells, we performed mass-spectrometric analysis of nucleotide composition of DNA. This method proved extremely reliable and reproducible including on known hypomethylated ES cell models (Supporting Information Fig. S1A). Analysis of pooled E7.5 epiblast and trophoblast tissue (as well as the intervening amnion, allantois, and chorion portion of the conceptus that consists of extraembryonic mesoderm, visceral ExEnd, and trophoblast) confirmed that total 5mC levels in trophoblast were only 56% of that in epiblast (Fig. 1B).

We also analyzed three independent ES, EpiSC, TS, and XEN cell lines and found that global DNA methylation levels were extremely concordant within each stem cell type and stable across a wide range of passages (>40 between the TS cell lines). Even between the different stem cell types, global 5mC content was very comparable at around 4% of total cytosine (Fig. 2B). Only XEN cells exhibited somewhat lower levels (70% of that in ES cells). 5mC levels in ES cells and EpiSCs were also very similar to those of epiblast tissue in vivo. The only prominent discrepancy was evident between TS cells and E7.5 trophoblast, as TS cells exhibited significantly higher methylation levels than their in vivo tissue counterpart. Since in vitro differentiation of TS cells was not accompanied by overt changes in total 5mC levels (Fig. 1B), this difference was unlikely caused by the differentiation stage of cells compared. However, this divergence might be partially due to elevated turnover rates of DNA methylation in trophoblast in vivo, as levels of 5-hydroxymethylcytosine (5hmC), one key oxidation product of 5mC [25, 26], were significantly higher in trophoblast than in TS cells (Fig. 1C).

Overall, 5hmC levels were very low in both extraembryonic stem cell types (i.e., TS and XEN cells). This correlated with very low expression levels of *Tet1* and *Tet2*, the two key enzymes responsible for 5hmC production in ES cells, in TS and XEN cells (Supporting Information Fig. S1B). Therefore, 5hmC seems to play a subordinate role in maintaining multipotency of the two extraembryonic stem cell types, in contrast to its close association with the pluripotent state of ES cells [21, 27–29].

Satellite Repeat Hypomethylation Is Preserved in Extraembryonic Stem Cell Types

Previous evidence has indicated that one of the key epigenetic differences between the embryonic and extraembryonic lineages resides in the relative hypomethylation of pericentromeric satellite repeats in trophoblast and ExEnd tissues [30, 31]. This difference correlates with the globally reduced 5mC levels in extraembryonic tissues (Fig. 1B). To investigate whether changes to repeat methylation levels may explain the increase of 5mC in TS cells compared to in vivo trophoblast, we assessed major and minor pericentromeric satellite repeats, as well as L1 and Intracisternal A-particle (IAP) elements. Concordant with their methylation levels in epiblast and trophoblast tissue, satellite methylation was high in ES cells and EpiSCs (84% and 81%, and 80% and 90% at major and minor satellite repeats, respectively) but much lower in TS cells (47% and 53%) (Fig. 1D; Supporting Information Fig. S1C–S1E). Thus, lineage-specific pericentromeric satellite repeat methylation differences are preserved in stem cells of the early embryo and do not account for the globally higher 5mC content of TS cells compared to trophoblast tissue in vivo.

An Extraembryonic Lineage-Specific Epigenetic Signature at Key Regulatory Elements

To identify the stem cell type-specific distribution of DNA methylation, we chose two cell lines of each type of different sex chromosome content (1X vs. 2X), immunoprecipitated methylated DNA with an antibody against 5mC and performed high-throughput Illumina sequencing (MeDIP-Seq) [32, 33]. This technique is efficient in detecting relative methylation differences, including at fragments of low-to-medium CpG content (Supporting Information Fig. S2). We obtained 20–32 million reads for each sample of which approximately 60% could be mapped back to the reference genome (Supporting Information Table S1). The remaining sequences were repeat elements that were analyzed separately and corroborated a lack of major methylation differences at prominent repeat classes except satellite repeats (Supporting Information Fig. S2D).

We first focused on analyzing the distribution of methylation on autosomes. When using in silico designed 5 kb probes spaced 20 kb apart (thus representing one-fifth of the genome), all cell lines of the same stem cell type (Supporting Information Figs. S2E and S3A), and even those representing different lineages (Fig. 2A), exhibited an overall very similar distribution of DNA methylation throughout the genome. Analysis of various genomic features for methylation enrichment also showed a fairly comparable pattern between all cell lines. Coding and regulatory regions were more highly enriched, indicative of relative hypermethylation, and intergenic regions under-represented and hence globally hypomethylated (Fig. 2B).

The greatest differences between cell lines were observed in the proportion of reads aligning to autosomal CpG islands (CGIs) (Figs. 2C, 2D), suggesting that CGI methylation may be an indicator of stem cell type and lineage identity. Overall, TS and XEN cells were hypermethylated at CGIs compared to stem cells of the embryonic lineage, in particular ES cells (Fig. 2C). This was observed both when using bioinformatically defined high-CpG content CGIs, as well as a more recent, extended annotation of CGIs based on CXXC-motif protein binding [34, 35] that include less CpG-rich CGIs which are of particular developmental relevance [36, 37]. The CGI methylation profile was largely shared between both cell lines of each stem cell type and stably maintained across a wide range of passages (Fig. 2D; Supporting Information Table S2). Importantly, the CGI methylation landscape proved to be a defining feature that was clearly distinct between
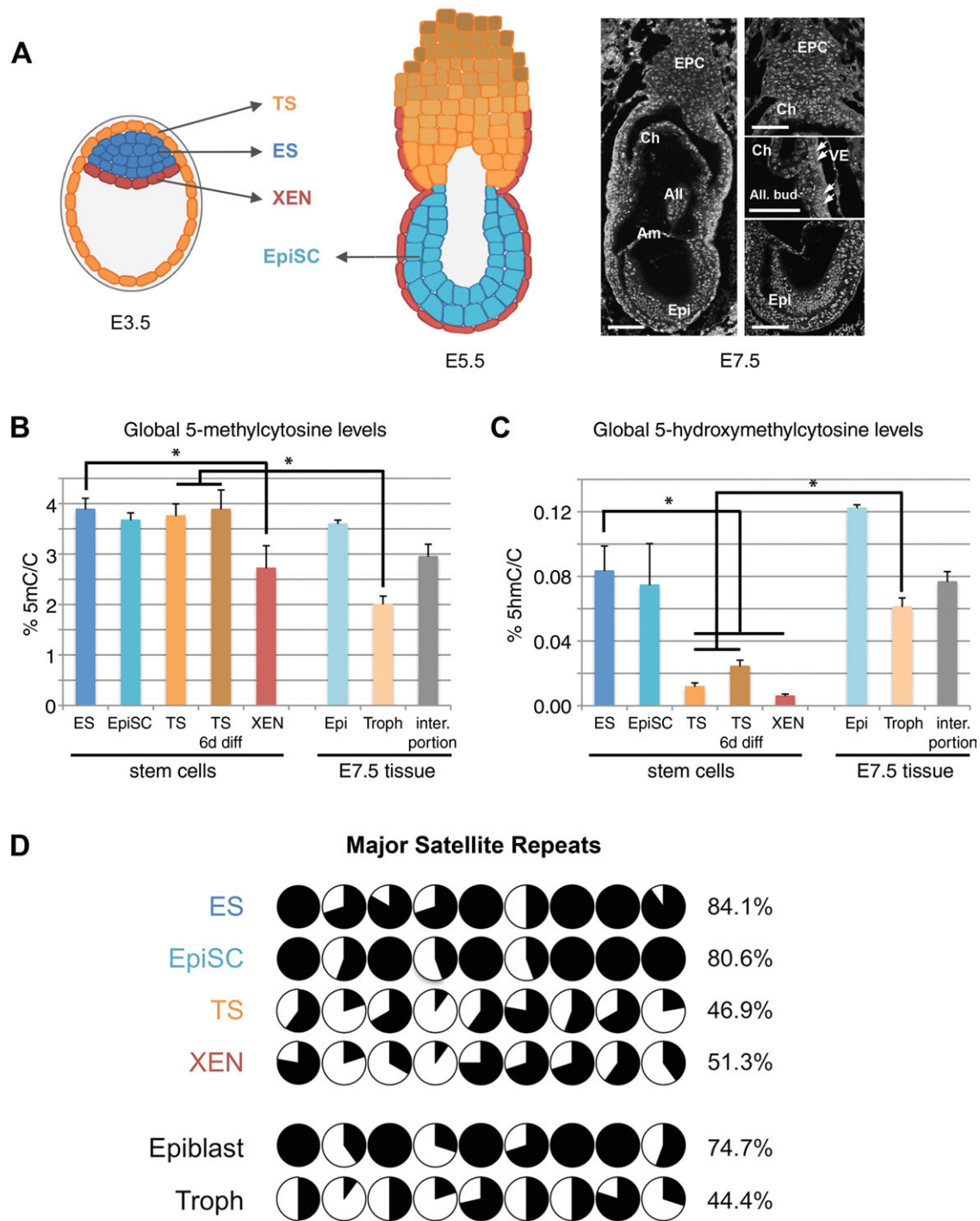
Figure 1. Global methylation analysis of stem cell types derived from early embryos. **(A):** Schematic representation of an E3.5 blastocyst and an E5.5 postimplantation embryo, and the stem cell types that can be derived from different cell lineages. Orange: trophoblast lineage, represented by trophectoderm at E3.5, and extraembryonic ectoderm and ectoplacental cone thereafter; blue: presumptive epiblast cells of the inner cell mass, red: primitive endoderm at E3.5 and visceral endoderm at E5.5, turquoise: epiblast. Confocal images of E7.5 conceptus stained for 5-mC, revealing slightly more intense staining of epiblast cells. VE (arrows) cells are somewhat heterogeneous in staining intensity. Magnification bars: 100 μm. **(B, C):** Global levels of 5mC (in (B)) and 5hmC (in (C)) expressed as a percentage of total C, as assayed by mass spectrometry of three independent cell lines of each stem cell type. In vivo tissues assessed are pooled E7.5 epiblast (Epi), ectoplacental cone trophoblast (Troph) and the intervening region (inter. portion) of the conceptus comprised amnion, allantois, and chorion (containing extraembryonic mesoderm, visceral ExEnd, and trophoblast). Key differences of statistical significance between pairwise comparisons (analyzed by Students' t test) are indicated. In (B), ES, EpiSC, TS, and TS 6d diff are not statistically different from each other; ES cell values are statistically different from XEN cells; TS and 6d in vitro differentiated TS cells are different from in vivo trophoblast tissue. In (C), ES cells are statistically different from TS, TS 6d diff, and XEN cells; EpiSCs are also different from TS and XEN cells; moreover, TS and TS 6d diff cells are different from in vivo trophoblast. **(D):** Summary of bisulphite sequencing analysis of major pericentromeric satellite repeats. Individual pie charts depict mean methylation per CpG dinucleotide from a minimum of 10 clones; total average methylation levels are given. Abbreviations: All, allantois; Am, amnion; Ch, chorion; Epi, epiblast; EPC, ectoplacental cone; ES, embryonic stem cells; EPC, ectoplacental cone; EpiSC, epiblast stem cell; troph, trophoblast; TS, trophoblast stem cells; VE, visceral endoderm; XEN, extraembryonic endoderm stem cells; 5mC, 5-methylcytosine; 5hmC 5-hydroxymethylcytosine.
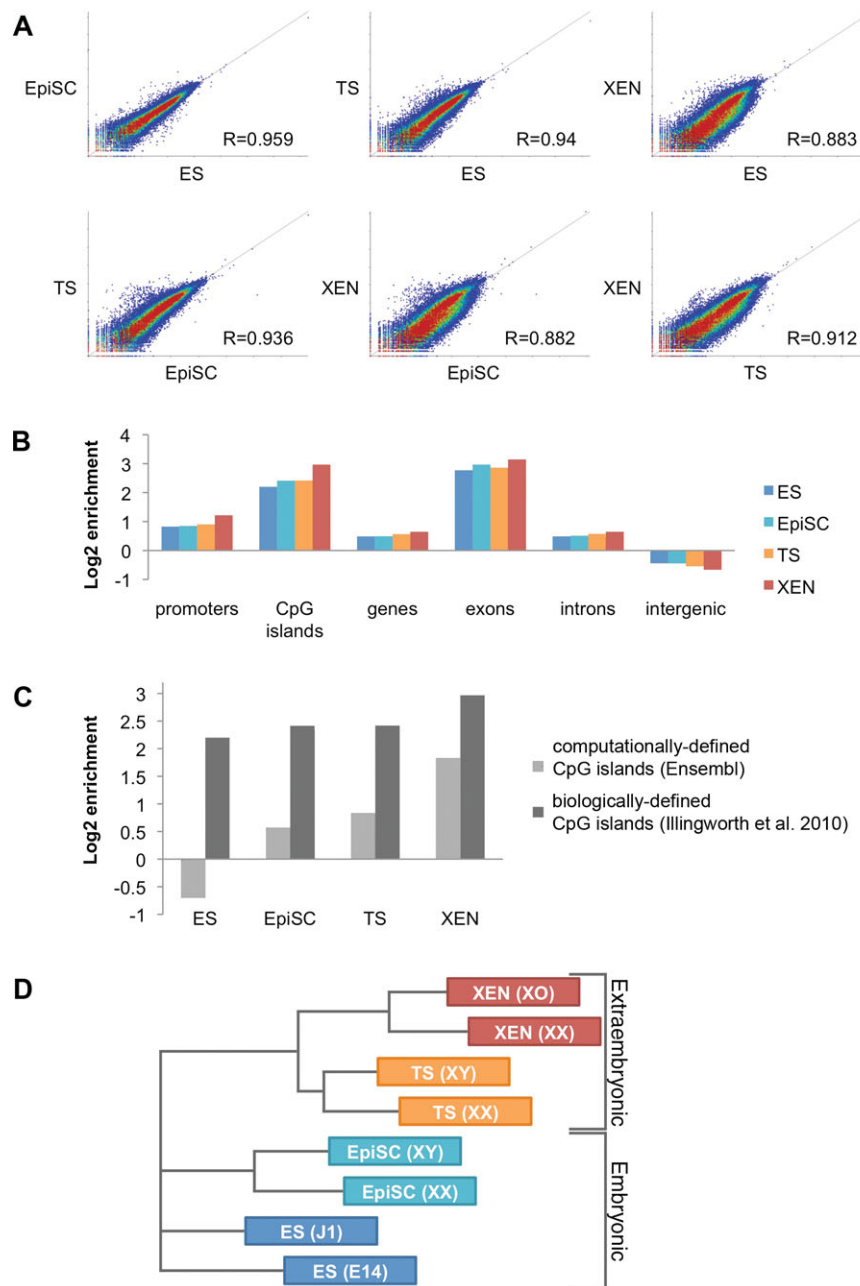
Figure 2. Methylomes of the four distinct stem cell types of the early embryo. **(A):** Scatter plots displaying Pearson's correlation of global methylation between each stem cell type. Each point corresponds to a 5 kb in silico probe spaced 20 kb apart. Values were normalized for total read count and converted to a Log_2 scale. **(B):** Graph showing the relative enrichment ($\log_2$% reads/% genome) of different genomic features for all the stem cell types. The CpG island annotation used is according to Illingworth et al. [35]. **(C):** Comparison of enrichment values for CpG islands using a bioinformatic annotation based on GC density (Ensembl annotation) or a "biological" annotation based on CXXC motif protein binding that is more likely to contain developmentally regulated CpG islands [35]. Note that overall enrichment values are higher for the biologically defined CpG islands that include sequences of lower GC density and comprise a considerably larger fraction of the genome. Importantly, however, the relative patterns of enrichment between the various cell lines are similar in both annotations, with lowest values in ES cells and highest in XEN cells. **(D):** A neighbor joining tree based on a Pearson's correlation distance matrix of autosomal CpG island methylation profiles clusters the two cell lines of each stem cell type together, indicating the close similarity of global methylation patterns within each stem cell pair. It also reveals a closer similarity of the extraembryonic stem cell types (TS and XEN) to each other than to the embryonic stem cell types (ES and EpiSC). Abbreviations: ES, embryonic stem cells; EpiSC, epiblast stem cells; TS, trophoblast stem cells; XEN, extraembryonic endoderm stem cells.

different stem cell types (Fig. 2D). TS and XEN cells were more similar to each other than to ES cells or EpiSCs, thus revealing an extraembryonic lineage-specific epigenetic signature at CGIs and at promoters (Supporting Information Fig. S3B) as key regulatory elements of transcriptional activity.

Embryonic Lineage-Specific Genes Are Tightly Methylated in Extraembryonic Stem Cell Types

Next we analyzed the datasets specifically for differentially methylated CGIs and promoters, using stringent parameters of fourfold differences shared between both stem cell lines of each
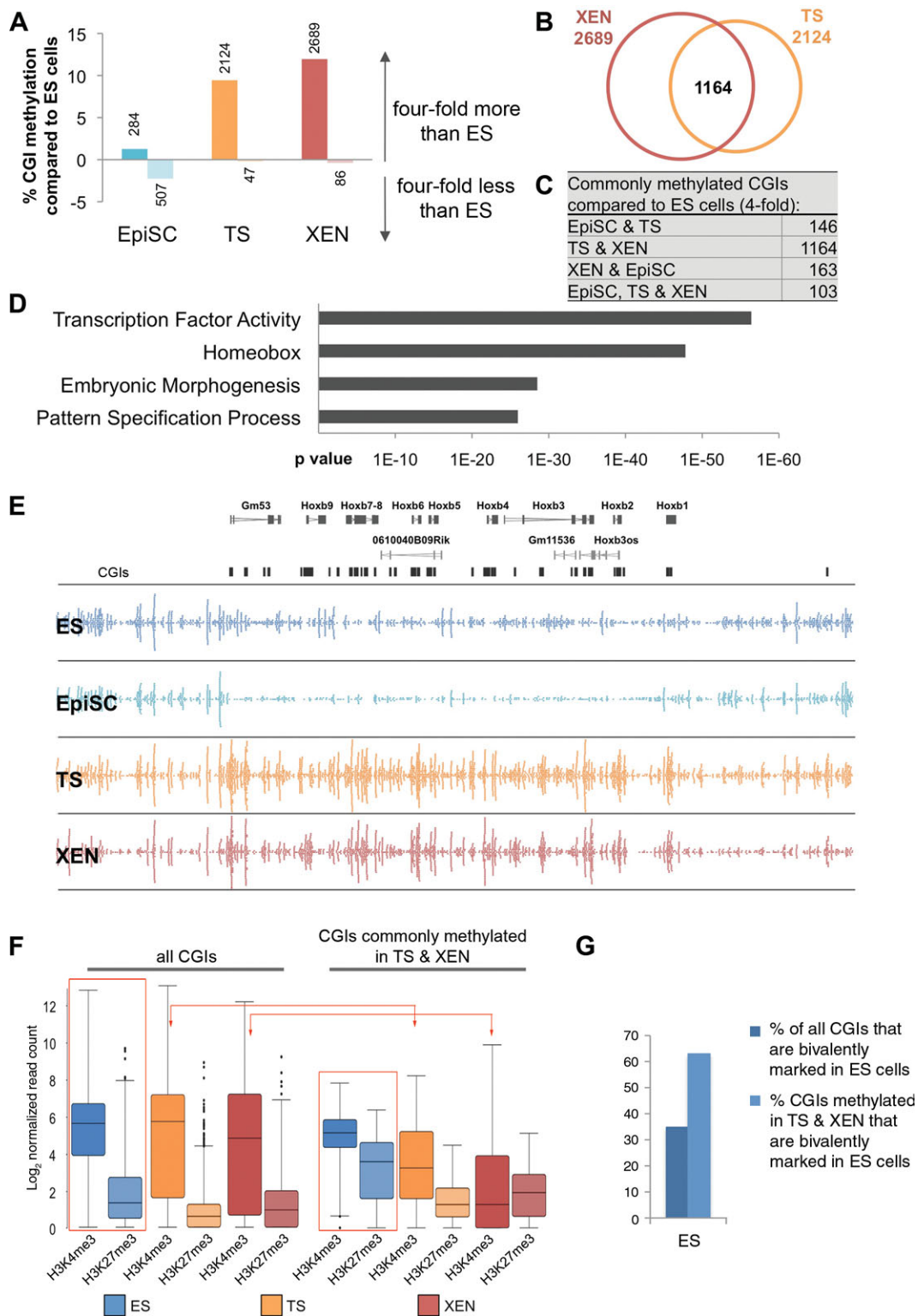
Figure 3. Epigenomic signature of extraembryonic lineages. **(A):** Graph showing the percentage of CGIs (Illingworth et al. [35]) with fourfold more or less reads compared to ES cells, indicative of relative hypermethylation and hypomethylation, respectively. CGI methylation of ES cells and EpiSCs is very similar, whereas many more CGIs are hypermethylated in TS and XEN cells. **(B):** Venn diagram illustrating the overlap of CGIs that are commonly hypermethylated in TS and XEN cells compared to ES cells, based on fourfold read count differences in each of the two stem cell lines of each type. **(C):** Table showing the numbers of CGIs that are commonly hypermethylated between different stem cell types compared to ES cells. For example, EpiSCs and TS cells share 146 CGIs that are more highly methylated in both of them than in ES cells. **(D):** Gene ontology analysis of genes associated (i.e., overlapping or within 500 bp downstream) with those CGIs that are commonly hypermethylated in both TS and XEN cells compared to ES cells. **(E):** Screen shot illustrating sequencing reads mapping to the *Hoxb* locus. Each data track displays the mean of the two individual stem cell lines of each type. **(F):** Combination of MeDIP-Seq datasets with H3K4me3 and H3K27me3 chromatin immunoprecipitation (ChIP)-Seq data [38]. Compared to the overall distribution of these histone marks at all CGIs, those CGIs that are methylated in TS and XEN cells (i.e., embryo-specific developmental regulators, Fig. 3D) are depleted for H3K4me3 (arrows) and enriched for H3K27me3, as expected from their silenced chromatin state. These same CGIs are enriched for both H3K4me3 and H3K27me3 in ES cells, indicative of their characteristic bivalent state in ES cells (red box). **(G):** Direct comparison of CGIs and bivalent chromatin marks in ES cells. Compared to the global level of bivalency across all CGIs, those CGIs that are methylated in TS and XEN cells are twofold enriched for the bivalent chromatin state in ES cells (light blue bar). This corroborates that these CGIs are predominantly associated with embryo-specific developmental regulators (that are bivalent in ES cells but methylated and repressed in TS and XEN cells). Abbreviations: CGI, CpG islands; ES, embryonic stem cells; EpiSC, epiblast stem cell; TS, trophoblast stem cells; XEN, extraembryonic endoderm cells.

type as a threshold, after normalization for global methylation levels (Fig. 1B). This screening method for differentially methylated sequence elements produced highly reliable results as we did not find any false positives. We assessed CGIs [35] and promoters on the whole and also subclassified them into promoter CGIs, intergenic CGIs, as well as non-CGI promoters (Fig. 3A; Supporting Information Fig. S3C). We found very little differences between ES cells and EpiSCs, with only a small number of CGIs hypermethylayed (1.3%) or hypomethylated (2.3%) in EpiSCs over ES cells. By contrast, many more CGIs were methylated in TS (9.4%) and XEN (12%) than in ES cells. This difference was more prevalent at intergenic CGIs, which may demarcate cryptic or alternative transcription initiation sites in extraembryonic tissues (Supporting Information Fig. S3C). Very few CGIs showed differential methylation in the opposite direction, that is, hypomethylated in TS and XEN cells over ES cells. This confirmed that promoters that are hypomethylated specifically in TS cells but hypermethylated in ES cells are rare, suggesting an exceptional role of genes, like *Elf5*, that are regulated in this way [17]. In fact, the small number of promoters that were more highly methylated in ES cells than in TS and particularly in XEN cells were enriched for non-CGI promoters (Supporting Information Fig. S3C). This finding may point to potential differences in the composition of the DNA methylation machinery in ES and extraembryonic stem cell types to preferentially target CpG-poor and CpG-enriched sequence elements, respectively.

The striking commonalities in epigenetic regulation between both extraembryonic stem cell types was further underpinned by the level of overlap of hypermethylated CGIs (Fig. 3B, 3C) and promoters (Supporting Information Fig. S3D–S3E) in TS and XEN cells. We found that 1,164 CGIs were commonly methylated in both stem cell types representing 55% and 43% of all differentially methylated CGIs in TS and XEN cells, respectively. The genes associated with these methylated CGIs were overwhelmingly enriched for homeobox genes (e.g., *Hox*, *Pax*, *Pou*, *Lhx* family members, *Pitx1*, *Gsc*), genes with transcription factor activity (e.g., *Zfp*'s, *Olig1*, *Olig2*, *Tead3*, *Sall1-3*, *Gli2*, *Sox13*), involved in pattern specification (e.g., *Lefty2*) and embryonic morphogenesis (e.g., *Wnt*'s, *Fgf*'s) (Fig. 3D). This pattern was exemplified at the *Hoxb* cluster where methylation peaks overlapped CGIs in TS and XEN cells but were largely absent from ES cells and EpiSCs (Fig. 3E). The same gene ontology enrichments were observed for the 164 promoters commonly methylated in TS and XEN cells (Supporting Information Fig. S3D–S3F). By comparing our MeDIP-Seq profiles with previously published H3K27me3 and H3K4me3 ChIP-Seq data [38], we also found that CGIs methylated in TS and XEN cells are relatively depleted for the activating H3K4me3 mark, as expected (Fig. 3F). Furthermore, these same CGIs that are silenced in extraembryonic tissues are mostly bivalently marked in ES cells, in line with them being associated with genes controlling embryonic development (Fig. 3G). Therefore, collectively, a picture emerges where developmental regulators that are poised for activation during embryogenesis are hypomethylated (and bivalent) in ES cells but are methylated and stably repressed in TS and XEN cells where their expression will not be required.

Lineage-Specific Methylation Marks Are Highly Reinforced in Extraembryonic Stem Cells In Vitro

We confirmed TS and XEN cell-specific hypermethylation at several loci of varying CpG content by Sequenom MassARRAY analysis (Fig. 4A; Supporting Information Fig. S4). Although these loci were also more highly methylated in E7.5 trophoblast tissue compared to epiblast, the extent of methyla-

tion was much less pronounced than in TS cells (Fig. 4A). The same pattern was also observed for the pluripotency factor OCT4 (encoded by the *Pou5f1* gene; Fig. 4B). A similar acquisition of methylation marks occurred between yolk sac ExEnd tissue and XEN cells (Fig. 6). Expression analysis of the DNA methyltransferases *Dnmt1*, *Dnmt3a*, and *Dnmt3b* indicated that this reinforcement is likely caused by continued high expression levels of *Dnmt3b* in TS cells compared to in vivo trophoblast (Fig. 4C). However, conversely, methylation levels in epiblast were comparable to those in ES cells and EpiSCs, as indicated by total 5mC content (Fig. 1B) and methylation levels at the trophoblast gene *Elf5* (Fig. 4B).

Imprinted X Inactivation Is Associated with CGI Methylation in Extraembryonic Stem Cells

The same phenomenon of an accumulation of DNA methylation was observed on the inactive X chromosome in the extraembryonic stem cells (TS, XEN) which undergo imprinted X inactivation (XCI; Fig. 5A). Unlike random XCI in the embryo proper that is associated with robust CGI methylation of X-linked genes, the inactive X chromosome in extraembryonic tissues has long been believed to be hypomethylated. Gene-specific analyses, as well as the expression of transgenes, have indicated that methylation is variable between loci and clearly not as prominent, widespread and critical for imprinted XCI maintenance in extraembryonic tissues [39–42]. However, in our analysis X-linked promoters and CGIs were highly enriched in XX EpiSC as well as XX TS and XEN cell lines, but not in those cell lines with only one X chromosome or in XX ES cells that have two active X chromosomes (Fig. 5B). This result indicates that X-linked CGIs are indeed methylated on the inactive X chromosome in TS and XEN cells, as well as in EpiSCs. Furthermore, when using X-linked CGIs for closest neighbor analysis, the XX cell lines clustered together regardless of stem cell type (Fig. 5C). This shared CGI methylation pattern indicates a common epigenetic regulation in both random and imprinted XCI.

When we validated these results by Sequenom MassARRAY for three X-linked promoter CGIs (*Pgk1*, *Smc1a*, and *Atp6*) we found that all XX cells exhibited methylation levels comparable to those in female fibroblasts and greater than their male counterparts (Fig. 5D). We also observed methylation at these CGIs in E7.5 female embryos. However, in trophoblast tissues, these loci were only slightly more methylated in E7.5 female than male EPC. Thus, as observed at autosomal CGIs, DNA methylation is also acquired on the inactive X chromosome during in vitro derivation of TS cells.

An Extraembryonic Cell Type-Specific Epigenetic Barrier

While TS and XEN cells share an epigenetic signature at CGIs and promoters to stabilize the repressed state of embryonic genes, specific DNA methylation hallmarks also set these two extraembryonic cell lineages apart. Key trophoblast transcription factors such as *Cdx2*, *Tfap2c*, *Elf5*, and *Eomes* were strongly methylated in XEN cells, while transcription factors important for ExEnd such as *Sox17*, *Gata6*, and *Sox7* were methylated in TS cells (Fig. 6A; Supporting Information Fig. S5B). We confirmed differential methylation of *Cdx2*, *Tfap2c*, and *Elf5* between TS and XEN cells by Sequenom MassARRAY analysis (Fig. 6B). To assess whether these genes were also methylated in a lineage-specific pattern in vivo, we analyzed Reichert's membrane consisting of parietal ExEnd to which XEN cells preferentially contribute. Methylation was absent from *Cdx2*, low at *Tfap2c*, and robust at *Elf5*, demonstrating the exquisite role of epigenetic regulation of *Elf5* for lineage specification (Fig. 6C; Supporting Information Fig. S5C).
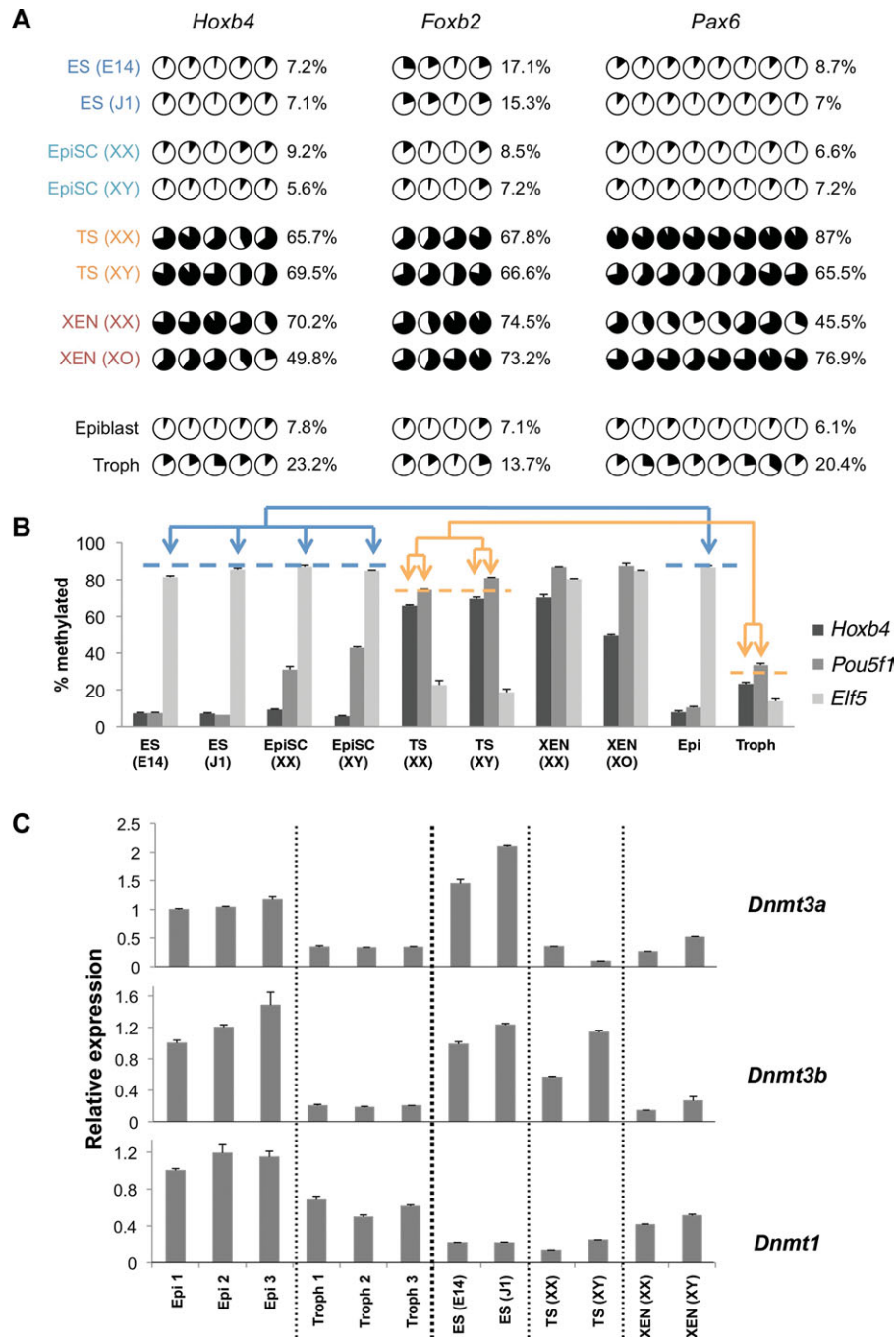
Figure 4. Methylation reinforcement in extraembryonic stem cells. **(A):** Sequenom MassARRAY analysis of *Hoxb4*, *Foxb2*, and *Pax6* promoter CpG islands (CGIs) in all stem cell types as well as E7.5 epiblast and trophoblast (Troph) tissue. Total average methylation percentages are given. Each pie chart shows the average methylation of a particular CpG unit from triplicate experiments. Note that pie charts do not necessarily represent consecutive CpGs as some CpGs within a given amplicon will be refractory to analysis by this method. **(B):** Comparison of *Hoxb4*, *Pou5f1*, and *Elf5* promoter methylation in all stem cell types as well as E7.5 epiblast (Epi) and trophoblast (Troph). Total average methylation levels determined by Sequenom MassARRAY analysis performed in triplicate are shown ± SEM. Methylation levels of *Elf5* are similar in ES cells, EpiSCs, and in vivo epiblast tissue (blue lines). In contrast, methylation of *Pou5f1* and *Hoxb4*—albeit present in trophoblast in vivo—is much higher in TS cell lines (orange lines). **(C):** Expression of *Dnmt* enzymes analyzed by RT-qPCR in three individual epiblast (Epi) and trophoblast (Troph) tissues, and the indicated stem cell lines. Abbreviations: ES, embryonic stem cells; EpiSC, epiblast stem cells; Epi, epiblast; Troph, trophoblast; TS, trophoblast stem cells; XEN, extraembryonic endoderm cells.

Collectively, these data show that embryonic lineage-specific de novo methylation is robust and maintained throughout ES and EpiSC cell culture. In contrast, TS and XEN cells acquire additional methylation in a lineage-specific pattern early during the stem cell derivation process, which is stably main-tained thereafter (Supporting Information Table S2). It is important to note that neither did we find any evidence of aberrant DNA methylation at loci thought to be active in TS and XEN cells nor did we observe further increases in DNA methylation over prolonged stem cell culture periods (Figs. 1B, 2D). This
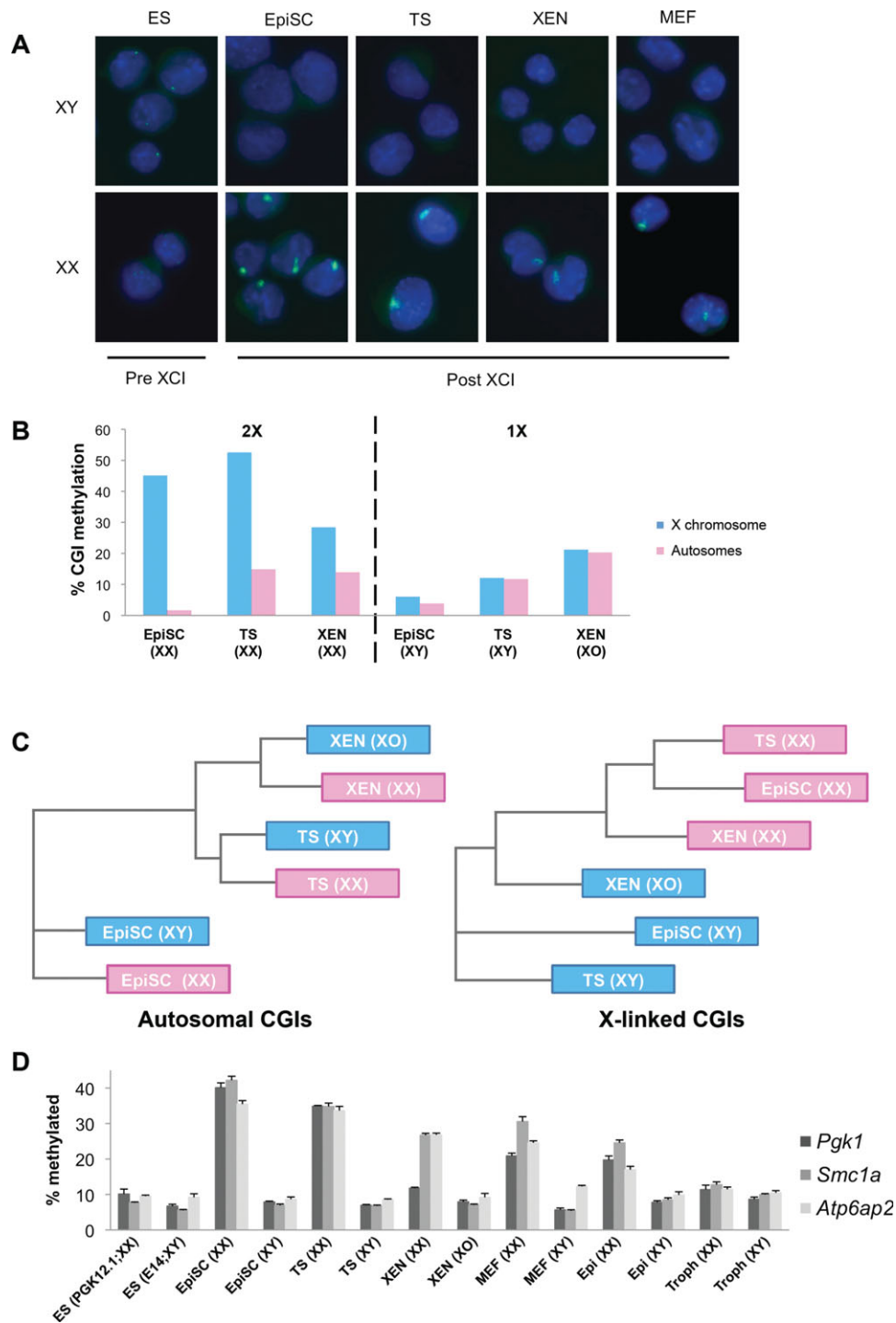
Figure 5. CGI methylation of X-linked genes in imprinted X inactivation in extraembryonic stem cells. **(A):** RNA-Flourescence in situ hybrid-isation (FISH) showing *Xist* RNA localization (green) in the various stem cell lines with different sex chromosome complements. DNA was coun-terstained with 4',6-diamidino-2-phenylindole (DAPI) (blue). **(B):** Graph showing percentage CGIs with fourfold more MeDIP-Seq reads compared to ES cells on autosomes and the X chromosome. Data have been normalized for X chromosome number. Higher methylation levels on the X chromosome in XX versus XY/XO cells indicates methylation of the inactive X chromosome. **(C):** Neighbor joining trees based on a Pearson's correlation distance matrix of autosomal and X-linked CGIs. Whereas the autosomal CGI comparison indicates high similarity between the two cell lines of each stem cell type (and the two extraembryonic lineages), the X-linked CGI comparison clusters cell lines with the same X chromosome complement together. **(D):** Sequenom MassARRAY validation of the methylation status of three X-linked promoter CGIs *Pgk1*, *Smc1a*, and *Atp6ap2* in stem cell lines as well as MEFs and E7.5 male and female epiblast (Epi) and trophoblast (Troph). Data are form triplicate experiments and shown as mean ± SEM. Abbreviations: CGI, CpG islands; ES, embryonic stem cells; EpiSC, epiblast stem cell; Epi, epiblast; MEF, mouse embryonic fibroblasts; TS, trophoblast stem cells; Troph, trophoblast; XEN, extraembryonic endoderm cells; XCI, X inactivation.
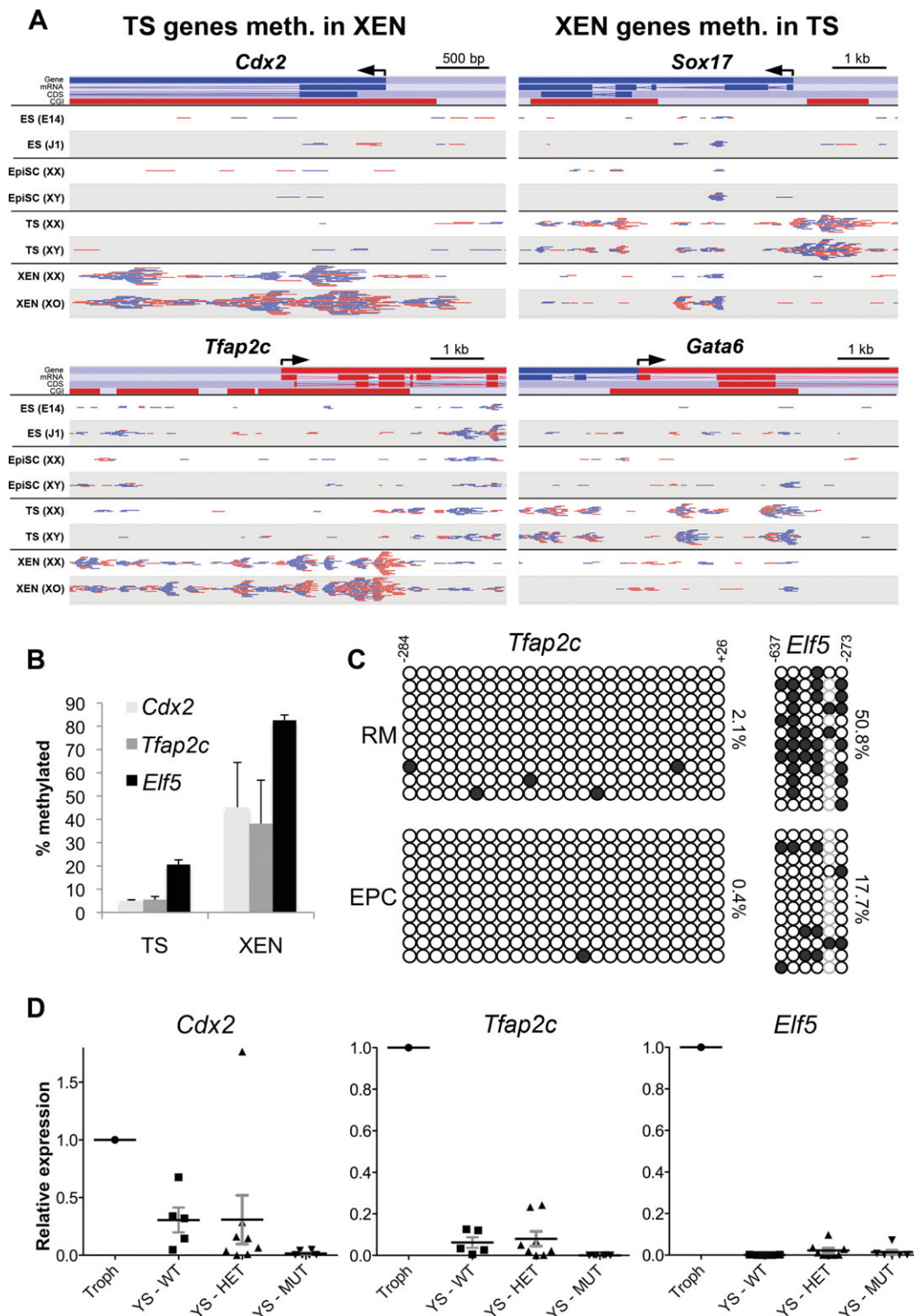
Figure 6. DNA methylation also establishes an epigenetic barrier between the two extraembryonic lineages. **(A):** Screenshots of MeDIP-Seq profiles of trophoblast transcription factors *Cdx2* and *Tfap2c* that are heavily methylated in XEN cells, and XEN transcription factors *Sox17* and *Gata6* that are methylated in TS cells. Horizontal red and blue lines show the number of reads indicative of higher methylation levels. The orientation of transcription is indicated by the arrow. **(B):** Sequenom MassARRAY analysis confirming higher methylation of trophoblast transcription factors *Cdx2*, *Tfap2c*, and *Elf5* in XEN cells. Average values of two cell lines analyzed for each stem cell type are shown (mean ± SEM). **(C):** In vivo methylation pattern, analyzed by bisulphite sequencing, of *Tfap2c* and *Elf5* in RM and EPC of E7.5 conceptuses, which represent tissues of the extraembryonic endoderm and trophoblast lineage, respectively. Note that the fifth CpG dinucleotide in the *Elf5* amplicon is polymorphic. Differential methylation is observed in these in vivo tissues in particular at *Elf5* but is not as pronounced as in the stem cell lines. **(D):** RT-qPCR analysis of trophoblast transcription factor expression in YS of *Dnmt1* WT, HET, and MUT conceptuses. Values from triplicate experiments per sample are shown relative to trophoblast expression levels. Abbreviations: EPC, ectoplacental cone; HET, heterozygous; MUT, mutant; RM, Reichert's membrane; TS, trophoblast stem cells; WT, wild-type; XEN, extraembryonic endoderm stem cells; YS, yolk sacs.
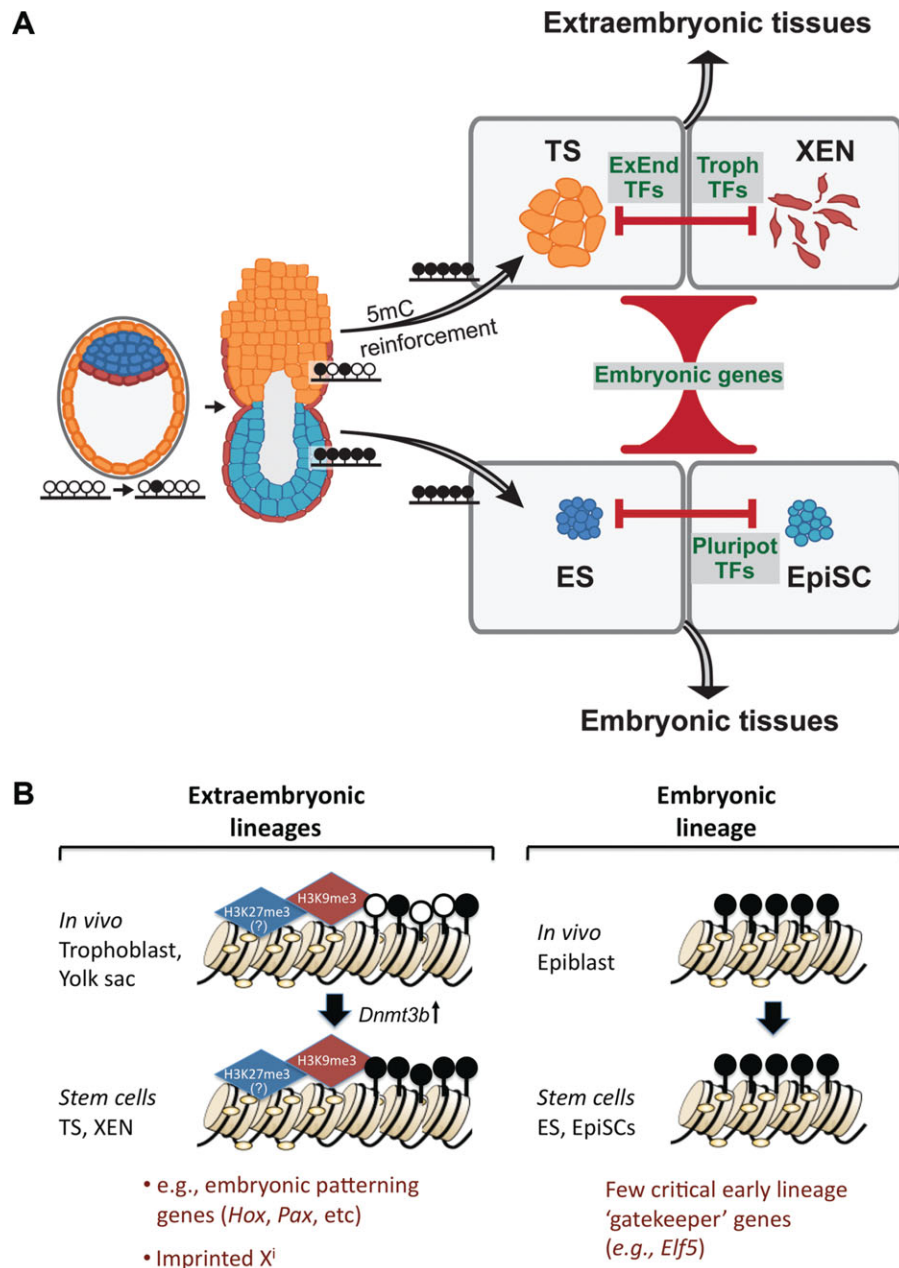
Figure 7. Model: Epigenetic lineage barriers established by DNA methylation define early embryo-derived stem cell types. **(A):** DNA methylation functions in cell lineage commitment from the mid-to-late blastocyst stage onward when de novo methylation peaks [15]. Stable epigenetic lineage barriers are established between the embryonic and extraembryonic lineages by methylation, for example, of embryonic patterning and morphogenesis genes. Reciprocal methylation of lineage-determining transcription factors distinguishes the trophoblast from the ExEnd lineage. Some pluripotency factors such as *Dppa3* [18] become methylated in the transition from the naïve to the primed state of pluripotency to distinguish ES cells from EpiSCs. Methylation becomes fully established in the postimplantation epiblast with similar levels as those in ES cells and EpiSCs. **(B):** In the embryonic lineage, robust DNA methylation of few important lineage "gatekeeper" genes is fully established in the postimplantation epiblast and equally in ES cells and EpiSCs. In the two extraembryonic lineages, multiple layers of epigenetic repressive marks ensure tight silencing of embryo-specific patterning and morphogenesis genes, as well as the imprinted X chromosome. DNA methylation is a relatively late, progressive acquisition, in line with its function in stabilizing the silent chromatin state to ensure lineage commitment. In the respective stem cells (TS and XEN), additional DNA methylation marks are laid down at these loci, most likely due to the continued presence of DNMT3B. Abbreviations: ES, embryonic stem; EpiSC, epiblast stem cell; TS, trophoblast; XEN, extraembryonic endoderm; TFs, transcription factors; 5mC, 5-methylcytosine.

hypermethylation affects embryonic genes that are already epigenetically repressed by H3K9me3, H3K27me3 as well as some DNA methylation [43, 44]. In line with such multilayered epigenetic repression, hypomethylation due to lack of *Dnmt1* [45] was not sufficient to activate these genes in trophoblast or ExEnd (Fig. 6D; Supporting Information Fig. S5A).

DISCUSSION

DNA methylation is essential for normal development [16, 46, 47], ensuring the progressive canalization of developmental pathways toward stable terminal differentiation. The

importance of the distribution of DNA methylation and how it changes during cellular differentiation has been well recognized in ES cells [48, 49] but its targets in other stem cell types, specifically those representing the extraembryonic lineages, remain poorly characterized. In this study, we generated genome-wide DNA methylation profiles of ES, EpiSC, TS, and XEN cells and identified a unique and distinctive methylation signature that defines each of these early embryo-derived stem cell types. This unbiased methylation survey significantly advances our previous microarray-based analysis that was limited to promoter elements in ES and TS cells [50]. It reveals important control elements of tissue- and cell type-specific transcriptional regulation in a comparative manner between all four stem cell types of the early embryo, with important implications for their cell lineage associations. We find that despite their distinct developmental origin, the two extraembryonic stem cell types share key epigenomic characteristics, most notably robust DNA methylation of embryo-specific developmental regulators as well as a subordinate role of 5-hydroxymethylation. This epigenetic signature forms a major epigenetic boundary between stem cells representative of the embryonic and the two extraembryonic lineages (Fig. 7A). While this boundary is the most prevailing feature of the methylome comparisons, DNA methylation also establishes heritable epigenetic barriers between the two extraembryonic stem cell types, notably by reciprocally targeting key lineage-determining transcription factors.

Our MeDIP procedure was powerful in detecting methylation differences at relatively CpG-poor regions such as the *Elf5* and *Nanog* promoters, but the most prominent DNA methylation changes were localized to CGIs. Recent insights into CGI biology has demonstrated that most, if not all, CGIs are sites of transcription initiation [35, 36, 51]. Although most CGIs are hypomethylated, CGIs not associated with annotated promoters (so-called orphan CGIs) are methylated much more frequently in a cell-, tissue- and differentiation-stage specific manner to regulate gene activity and transcript isoform expression and, consequently, cell fate [51–53]. Our analysis identified a large cohort of CGIs differentially methylated in the various stem cell types, with a predominance of orphan CGIs. They will be most valuable to uncover novel control elements and pivotal gatekeeper genes in stem cell potency and lineage differentiation, such as *Pdzd3* and *Klk1b11* as candidates for having important roles in the ExEnd (Supporting Information Fig. S5B).

A general feature of all stem cell types is that they acquire methylation during derivation and culture. This is consistent with previous reports of characteristic and reproducible hypermethylation events, for example, during neural precursor cell culture [49]. Similarly, the promoter methylation profile of mouse ES cells is more akin to that of postimplantation epiblast tissue than to blastocyst stage embryos from which they are derived [54]. Our mass spectrometric assessment extends this observation to the genome-wide level as we identified similar total 5mC levels in ES cells, EpiSCs, and epiblast tissue. In contrast, we find a striking discrepancy between methylation levels of TS cells and trophoblast tissues of the postimplantation conceptus. This difference is most likely caused by the hypermethylation of embryo-specific genes in extraembryonic stem cells. This acquisition of methylation is already evident in relatively early-passage TS cells (P14), is stably maintained thereafter (P56), and occurs in a highly stem cell type-specific pattern, demonstrating that it does not represent a progressive accumulation of stochastic "aberrant" methylation over extended culture. Instead, already repressed genes further accumulate DNA methylation in TS and XEN cells, presumably through continued high expression levels of *Dnmt3b* (Fig. 7B). This finding is perfectly in line with the view that CGI methyl-

ation does not appear to initiate gene repression but rather functions to stabilize the silent state [17, 36, 44]. *Dnmt3b* is expressed at the late blastocyst stage in the PE and polar TE, but is rapidly downregulated upon trophoblast differentiation ([55]; and data not shown). Therefore, it is likely that the short lifespan of a TS (and XEN) progenitor cell in vivo prohibits the establishment of solid methylation patterns. It should be noted, however, that the acquisition of DNA methylation and apparent loss of 5-hydroxymethylation compared to in vivo trophoblast tissue may also indicate that perhaps routine culture conditions used for TS (and XEN) cell maintenance are suboptimal to retain their full developmental potential, which may explain the relatively low contribution rate of TS cells to placental tissues in chimeras [8, 56, 57].

CGI silencing can occur not only through dense CpG methylation but also through Polycomb recruitment [58]. Redundancy in epigenetic repressive mechanisms seems particularly prevalent in extraembryonic tissues to keep embryo-specific developmental regulators stably shut off. These embryonic genes are typically in a bivalent chromatin state poised for activation in ES cells [59–61] but are silenced in extraembryonic tissues through addition of H3K9me3 to create a repressive "trivalent" H3K4me3/H3K27me3/H3K9me3 histone mark. In addition, they also progressively acquire DNA methylation to permanently "lock in" the repressed state [43, 44]. As a consequence of these multiple layers of epigenetic repression, removal of neither H3K9me3 [43] nor DNA methylation alone (Fig. 6D; Supporting Information Fig. S5A) is sufficient to reactivate expression of these genes in trophoblast and yolk sac tissues. This observation is further corroborated by the expression profile of *Dnmt1/3a/3b* triple-null TS cells that do not globally upregulate embryonic genes [57]. The synergistic function of multiple epigenetic repressive mechanisms explains why DNA methylation is seemingly dispensable in trophoblast cells [57]. Thus stable repression of embryo-specific genes in extraembryonic tissues is one of the most distinctive features that sets early cell lineages apart.

Our analysis revealed a striking epigenetic coregulation of the two extraembryonic lineages (Fig. 7A) characterized by globally similar promoter and CGI methylation profiles, satellite repeat hypomethylation and the discussed enforcement of embryo-specific gene silencing by multiple epigenetic repressive mechanisms. Epigenetic coregulation of the extraembryonic lineages is well known at the locus- or chromosome-specific level, for example, by hypomethylation of repeat elements [30], imprinted XCI [62], and imprinted gene regulation [63]. A shared extraembryonic lineage regulation has been observed recently also in the expression profiles of microRNAs [64]. Here, we extend these insights and report significant overlaps in the global distribution of DNA methylation, corroborating the idea of a commonality in epigenetic regulation of both lineages. This shared regulation is developmentally intriguing as TE cells are the first to be set apart in the morula-to-blastocyst transition, whereas PE cells are the last to delaminate from a common pool of cells within the ICM [1]. Although gene expression differences have been described between future PE and epiblast cells within the ICM [65, 66], our findings suggest that these future PE cells may be already epigenetically pre-determined before they become morphologically distinct.

CONCLUSION

Taken together, we here show that global DNA methylation patterns are a defining feature of each stem cell type that

underpin lineage commitment and differentiative potency of early embryo-derived stem cells. Our detailed methylation profiles identify a distinct cohort of epigenetically regulated sequence elements, most notably orphan CGIs, that will be most valuable to uncover novel transcriptional regulators and pivotal gatekeeper genes in stem cell potency and lineage differentiation.

ACKNOWLEDGMENTS

DISCLOSURE OF POTENTIAL CONFLICTS OF INTEREST

The authors indicate no potential conflicts of interest.

REFERENCES

1   Rossant J, Tam PP. Blastocyst lineage formation, early embryonic asymmetries and axis patterning in the mouse. Development 2009; 136:701–713.
2   Artus J, Hadjantonakis AK. Troika of the mouse blastocyst: Lineage segregation and stem cells. Curr Stem Cell Res Ther 2012;7:78–91.
3   Zernicka-Goetz M, Morris SA, Bruce AW. Making a firm decision: Multifaceted regulation of cell fate in the early mouse embryo. Nat Rev Genet 2009;10:467–477.
4   Dietrich JE, Hiiragi T. Stochastic patterning in the mouse pre-implantation embryo. Development 2007;134:4219–4231.
5   Rossant J. Stem cells and lineage development in the mammalian blastocyst. Reprod Fertil Dev 2007;19:111–118.
6   Arnold SJ, Robertson EJ. Making a commitment: Cell lineage allocation and axis patterning in the early mouse embryo. Nat Rev Mol Cell Biol 2009;10:91–103.
7   Evans MJ, Kaufman MH. Establishment in culture of pluripotential cells from mouse embryos. Nature 1981;292:154–156.
8   Tanaka S, Kunath T, Hadjantonakis AK et al. Promotion of trophoblast stem cell proliferation by FGF4. Science 1998;282:2072–2075.
9   Kunath T, Arnaud D, Uy GD et al. Imprinted X-inactivation in extraembryonic endoderm cell lines from mouse blastocysts. Development 2005;132:1649–1661.
10 Brons IG, Smithers LE, Trotter MW et al. Derivation of pluripotent epiblast stem cells from mammalian embryos. Nature 2007;448: 191–195.
11 Tesar PJ, Chenoweth JG, Brook FA et al. New cell lines from mouse epiblast share defining features with human embryonic stem cells. Nature 2007;448:196–199.
12 Kwon GS, Viotti M, Hadjantonakis AK. The endoderm of the mouse embryo arises by dynamic widespread intercalation of embryonic and extraembryonic lineages. Dev Cell 2008;15:509–520.
13 Beddington RS, Robertson EJ. An assessment of the developmental potential of embryonic stem cells in the midgestation mouse embryo. Development 1989;105:733–737.
14 Bradley A, Evans M, Kaufman MH et al. Formation of germ-line chimaeras from embryo-derived teratocarcinoma cell lines. Nature 1984; 309:255–256.
15 Santos F, Hendrich B, Reik W et al. Dynamic reprogramming of DNA methylation in the early mouse embryo. Dev Biol 2002;241: 172–182.
16 Reik W. Stability and flexibility of epigenetic gene regulation in mammalian development. Nature 2007;447:425–432.
17 Ng RK, Dean W, Dawson C et al. Epigenetic restriction of embryonic cell lineage fate by methylation of Elf5. Nat Cell Biol 2008;10: 1280–1290.
18 Hayashi K, Lopes SM, Tang F et al. Dynamic equilibrium and heterogeneity of mouse pluripotent stem cells with distinct functional and epigenetic states. Cell Stem Cell 2008;3:391–401.
19 Waddington CH. Organisers and Genes. Cambridge: Cambridge University Press, 1940.
20 Senner CE, Nesterova TB, Norton S et al. Disruption of a conserved region of Xist exon 1 impairs Xist RNA localisation and X-linked gene silencing during random and imprinted X chromosome inactivation. Development 2011;138:1541–1550.
21 Ficz G, Branco MR, Seisenberger S et al. Dynamic regulation of 5-hydroxymethylcytosine in mouse ES cells and during differentiation. Nature 2011;473:398–402.
22 Huang da W, Sherman BT, Lempicki RA. Systematic and integrative analysis of large gene lists using DAVID bioinformatics resources. Nat Protoc 2009;4:44–57.
23 Huang da W, Sherman BT, Lempicki RA. Bioinformatics enrichment tools: Paths toward the comprehensive functional analysis of large gene lists. Nucleic Acids Res 2009;37:1–13.
24 Nesterova TB, Popova BC, Cobb BS et al. Dicer regulates Xist promoter methylation in ES cells indirectly through transcriptional control of Dnmt3a. Epigenetics Chromatin 2008;1:2.
25 Tahiliani M, Koh KP, Shen Y et al. Conversion of 5-methylcytosine to 5-hydroxymethylcytosine in mammalian DNA by MLL partner TET1. Science 2009;324:930–935.
26 Kriaucionis S, Heintz N. The nuclear DNA base 5-hydroxymethylcytosine is present in Purkinje neurons and the brain. Science 2009;324: 929–930.
27 Ito S, D'Alessio AC, Taranova OV et al. Role of Tet proteins in 5mC to 5hmC conversion, ES-cell self-renewal and inner cell mass specification. Nature 2010;466:1129–1133.
28 Koh KP, Yabuuchi A, Rao S et al. Tet1 and Tet2 regulate 5-hydroxymethylcytosine production and cell lineage specification in mouse embryonic stem cells. Cell Stem Cell 2011;8:200–213.
29 Dawlaty MM, Ganz K, Powell BE et al. Tet1 is dispensable for maintaining pluripotency and its loss is compatible with embryonic and postnatal development. Cell Stem Cell 2011;9:166–175.
30 Chapman V, Forrester L, Sanford J et al. Cell lineage-specific undermethylation of mouse repetitive DNA. Nature 1984;307:284–286.
31 Oda M, Yamagiwa A, Yamamoto S et al. DNA methylation regulates long-range gene silencing of an X-linked homeobox gene cluster in a lineage-specific manner. Genes Dev 2006;20:3382–3394.
32 Weber M, Davies JJ, Wittig D et al. Chromosome-wide and promoter-specific analyses identify sites of differential DNA methylation in normal and transformed human cells. Nat Genet 2005;37:853–862.
33 Weber M, Hellmann I, Stadler MB et al. Distribution, silencing potential and evolutionary impact of promoter DNA methylation in the human genome. Nat Genet 2007;39:457–466.
34 Illingworth R, Kerr A, Desousa D et al. A novel CpG island set identifies tissue-specific methylation at developmental gene loci. PLoS Biol 2008;6:e22.
35 Illingworth RS, Gruenewald-Schneider U, Webb S et al. Orphan CpG islands identify numerous conserved promoters in the mammalian genome. PLoS Genet 2010;6:e1001134.
36 Deaton AM, Bird A. CpG islands and the regulation of transcription. Genes Dev 2011;25:1010–1022.
37 Blackledge NP, Long HK, Zhou JC et al. Bio-CAP: A versatile and highly sensitive technique to purify and characterise regions of non-methylated DNA. Nucleic Acids Res 2012;40:e32.
38 Rugg-Gunn PJ, Cox BJ, Ralston A et al. Distinct histone modifications in stem cell lines and tissue lineages from the early mouse embryo. Proc Natl Acad Sci USA 2010;107:10783–10790.
39 Dementyeva EV, Shevchenko AI, Anopriyenko OV et al. Difference between random and imprinted X inactivation in common voles. Chromosoma 2010;119:541–552.
40 Garrick D, Sharpe JA, Arkell R et al. Loss of Atrx affects trophoblast development and the pattern of X-inactivation in extraembryonic tissues. PLoS Genet 2006;2:e58.
41 Hadjantonakis AK, Cox LL, Tam PP et al. An X-linked GFP transgene reveals unexpected paternal X-chromosome activity in trophoblastic giant cells of the mouse placenta. Genesis 2001;29:133–140.
42 Sado T, Fenner MH, Tan SS et al. X inactivation in the mouse embryo deficient for Dnmt1: Distinct effect of hypomethylation on imprinted and random X inactivation. Dev Biol 2000;225:294–303.

43 Alder O, Lavial F, Helness A et al. Ring1B and Suv39h1 delineate distinct chromatin states at bivalent genes during early mouse lineage commitment. Development 2010;137:2483–2492.

44 Nakanishi MO, Hayakawa K, Nakabayashi K et al. Trophoblast-specific DNA methylation occurs after the segregation of the trophectoderm and inner cell mass in the mouse periimplantation embryo. Epigenetics 2012;7:173–182.

45 Lei H, Oh SP, Okano M et al. De novo DNA cytosine methyltransferase activities in mouse embryonic stem cells. Development 1996;122: 3195–3205.

46 Li E, Bestor TH, Jaenisch R. Targeted mutation of the DNA methyltransferase gene results in embryonic lethality. Cell 1992;69:915–926.

47 Bestor TH. The DNA methyltransferases of mammals. Hum Mol Genet 2000;9:2395–2402.

48 Lister R, Pelizzola M, Dowen RH et al. Human DNA methylomes at base resolution show widespread epigenomic differences. Nature 2009;462:315–322.

49 Meissner A, Mikkelsen TS, Gu H et al. Genome-scale DNA methylation maps of pluripotent and differentiated cells. Nature 2008;454: 766–770.

50 Farthing CR, Ficz G, Ng RK et al. Global mapping of DNA methylation in mouse promoters reveals epigenetic reprogramming of pluripotency genes. PLoS Genet 2008;4:e1000116.

51 Maunakea AK, Nagarajan RP, Bilenky M et al. Conserved role of intragenic DNA methylation in regulating alternative promoters. Nature 2010;466:253–257.

52 Zhou JC, Blackledge NP, Farcas AM et al. Recognition of CpG island chromatin by KDM2A requires direct and specific interaction with linker DNA. Mol Cell Biol 2012;32:479–489.

53 Deaton AM, Webb S, Kerr AR et al. Cell type-specific DNA methylation at intragenic CpG islands in the immune system. Genome Res 2011;21:1074–1086.

54 Borgel J, Guibert S, Li Y et al. Targets and dynamics of promoter DNA methylation during early mouse development. Nat Genet 2010; 42:1093–1100.

55 Hirasawa R, Sasaki H. Dynamic transition of Dnmt3b expression in mouse pre- and early post-implantation embryos. Gene Expr Patterns 2009;9:27–30.

56 Lu CW, Yabuuchi A, Chen L et al. Ras-MAPK signaling promotes trophectoderm formation from embryonic stem cells and mouse embryos. Nat Genet 2008;40:921–926.

57 Sakaue M, Ohta H, Kumaki Y et al. DNA methylation is dispensable for the growth and survival of the extraembryonic lineages. Curr Biol 2010;20:1452–1457.

58 Mendenhall EM, Koche RP, Truong T et al. GC-rich sequence elements recruit PRC2 in mammalian ES cells. PLoS Genet 2010;6: e1001244.

59 Boyer LA, Plath K, Zeitlinger J et al. Polycomb complexes repress developmental regulators in murine embryonic stem cells. Nature 2006;441:349–353.

60 Bernstein BE, Mikkelsen TS, Xie X et al. A bivalent chromatin structure marks key developmental genes in embryonic stem cells. Cell 2006;125:315–326.

61 Azuara V, Perry P, Sauer S et al. Chromatin signatures of pluripotent cell lines. Nat Cell Biol 2006;8:532–538.

62 Takagi N, Sasaki M. Preferential inactivation of the paternally derived X chromosome in the extraembryonic membranes of the mouse. Nature 1975;256:640–642.

63 Hudson QJ, Seidl CI, Kulinski TM et al. Extra-embryonic-specific imprinted expression is restricted to defined lineages in the post-implantation embryo. Dev Biol 2011;353:420–431.

64 Spruce T, Pernaute B, Di-Gregorio A et al. An early developmental role for miRNAs in the maintenance of extraembryonic stem cells in the mouse embryo. Dev Cell 2010;19:207–219.

65 Chazaud C, Yamanaka Y, Pawson T et al. Early lineage segregation between epiblast and primitive endoderm in mouse blastocysts through the Grb2-MAPK pathway. Dev Cell 2006;10:615–624.

66 Artus J, Piliszek A, Hadjantonakis AK. The primitive endoderm lineage of the mouse blastocyst: Sequential transcription factor activation and regulation of differentiation by Sox17. Dev Biol 2011;350: 393–404.

See www.StemCells.com for supporting information available online.